symmetry

MDPI

Article

Production Mechanism of the Charmed Baryon Λ_c^+

Weiping Wang [1,2,*], Xiaorong Zhou [1,2,*], Rinaldo Baldini Ferroli [3,*] and Guangshun Huang [1,2,*]

1 Modern Physics Department, University of Science and Technology of China, Hefei 230026, China
2 State Key Laboratory of Particle Detection and Electronics, Hefei 230026, China
3 INFN Laboratori Nazionali di Frascati, I-00044 Frascati, Italy
* Correspondence: weipingwang@ustc.edu.cn (W.W.); zxrong@ustc.edu.cn (X.Z.); Rinaldo.Baldini@lnf.infn.it (R.B.F.); hgs@ustc.edu.cn (G.H.)

Abstract: As the lightest charmed baryon, precision measurement of the pair production cross section of Λ_c^+ provides unprecedented experimental information for the investigation of baryon production mechanism. In addition, the extraction of the polar angle distributions of the outgoing Λ_c^+ in the annihilation of the electron–positron help to determine its electromagnetic form factors, which is currently the unique key to access the internal structure of the baryons. In this article, the measurement of $e^+e^- \to \Lambda_c^+\bar{\Lambda}_c^-$ process via the initial state radiation technique at Belle detector and direct electron–positron annihilation at BESIII with discrete center-of-mass energies near threshold are briefly reviewed. In addition, the electromagnetic form factor ratios of Λ_c^+ measured by BESIII are also investigated. A few theoretical models that parameterize the center-of-mass energy dependence of the cross section and electromagnetic form factors of baryon are introduced and the contributions of Λ_c^+ data to them are discussed.

Keywords: charmed baryon; form factors; threshold enhancement; charmed baryonium

Citation: Wang, W.; Zhou, X.; Ferroli, B.R.; Huang, G. Production Mechanism of the Charmed Baryon Λ_c^+. *Symmetry* **2022**, *14*, 5. https://doi.org/10.3390/sym14010005

Academic Editor: Maxim Yu. Khlopov

Received: 29 November 2021
Accepted: 14 December 2021
Published: 21 December 2021

1. Introduction

One of the challenging question in particle physics, how quarks and gluons form hadrons, has not been understood in experimental or theoretical points of view. However, the electromagnetic form factors (FFs), which are used to parameterize the internal electromagnetic structure of hadrons, have been studied since 1960s [1]. The nucleon, including the proton and neutron, which are the most abundant building blocks of the Universe, has been studied both in the space-like and time-like domains. Nowadays, the unprecedented data with larger statistics collected at electron–positron collision facilities brings the access to strange and charm hyperon structure [2]. Under the hypothesis that the one-photon exchange process dominates the production of spin-1/2 baryon B, the differential cross section of the time-like process $e^+e^- \to B\bar{B}$ is expressed in terms of electromagnetic FFs [3]:

$$\frac{d\sigma_{B\bar{B}}}{d\cos\theta}(s,\theta) = \frac{\pi\alpha^2\beta C}{2s}\left[|G_M(s)|^2(1+\cos^2\theta) + \frac{4m_B^2}{s}|G_E(s)|^2\sin^2\theta\right]. \quad (1)$$

where α is the fine-structure constant and s the square of the center-of-mass (c.m.) energy. The polar angle and velocity of the out-going baryon in the c.m. frame are denoted by θ and $\beta = \sqrt{1-4m_B^2c^4/s}$, respectively, where m_B is the mass of the baryon. As the linear combinations of the Dirac and Pauli form factors, the electric form factor G_E and magnetic form factor G_M are the functions of s [4]. As a consequence of the optical theorem, there are imaginary parts in both G_M and G_E as long as $s \geq 4m_\pi^2$. According to Equation (1), the module of electromagnetic FF ratio, i.e., $|G_E/G_M|$, is associated with the polar angle dependence of the baryon pair production rate and could be extracted by analyzing the polar angle distribution of the corresponding baryon. The Coulomb factor C parameterizes the electromagnetic interaction between the baryon and anti-baryon

produced from the virtual photon. For the neutral baryons such as neutron and strange hyperon Λ, the Coulomb factor equal to unity, while for point-like charged fermions $C = y/(1 - e^{-y})$ with $y = \pi\alpha\sqrt{1-\beta^2}/\beta$ [5–7].

After integrating over the polar angle θ in Equation (1), the total production cross section of baryon B at c.m. energy $\sqrt{s}$ takes the form

$$\sigma_{B\bar{B}}(s) = \frac{4\pi\alpha^2\beta C}{3s}\left[|G_M(s)|^2 + \frac{2m_B^2}{s}|G_E(s)|^2\right]. \quad (2)$$

For the charged spin-1/2 baryon, β in Equation (2) is canceled by that in the Coulomb factor at any c.m. energy; therefore, a non-zero cross section at the very beginning of the kinematic threshold of process $e^+e^- \to B\bar{B}$ is expected.

In this review, the production cross section and electromagnetic form factor ratios of the lightest charmed baryon Λ_c^+ are discussed based on the published results.

2. Previous Measurements

The first hint of a charmed baryon was observed in the interaction between a high-energy neutrino and the hydrogen in the cryogenic bubble chamber at Brookhaven National Laboratory [8], in which the decay process $\Sigma_c^{++} \to \Lambda_c^+\pi^+$ was believed to be the intermediate procedure related to the charmed baryons. Later on, the evidence of the lightest charmed baryon $\bar{\Lambda}_c^-$ was detected by combining the multi-hadron final states $\bar{\Lambda}\pi^-\pi^-\pi^+$ produced by wide-band photon beam at Fermilab [9]. The charmed baryon Λ_c^+ was firstly reconstructed via the final state hadrons p, K^- and π^+, which were produced by the electron–positron annihilation at MarkII detector in SLAC [10]. This *golden* channel is a Cabibbo-favored weak decay of Λ_c^+, which manifests itself since Λ_c^+ is the lowest-lying charmed baryon.

Exclusive pair production cross sections of Λ_c^+ was firstly measured by the Belle collaboration with the initial state radiation (ISR) technique at the KEKB asymmetric-energy electron–positron collider [11], in which the used data samples were taken at the $\Upsilon(4S)$ resonance and nearby continuum with an integrated luminosity of 569 fb^{-1}. Figure 1 shows the Feynman diagram for the ISR returned exclusive $\Lambda_c^+\bar{\Lambda}_c^-$ events.

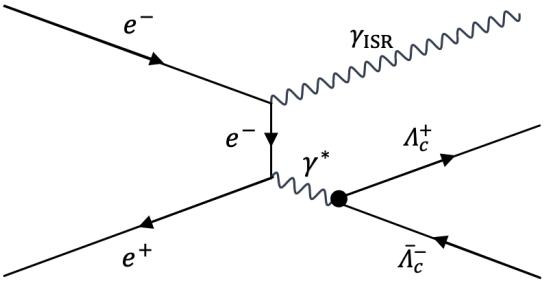

Figure 1. Feynman diagram of the process $e^+e^- \to \gamma_{\rm ISR}\Lambda_c^+\bar{\Lambda}_c^-$, where $\gamma_{\rm ISR}$ is the ISR photon radiated by the initial beam while γ^* denotes the virtual photon produced by electron–positron annihilation.

To measure the cross section from the $\Lambda_c^+\bar{\Lambda}_c^-$ kinematic threshold, a high-energy photon ($\sim$4.3 GeV) should be radiated by the initial electron or positron. Due to the highly suppressed probability of radiating a hard ISR photon, the process $e^+e^- \to \gamma_{\rm ISR}\Lambda_c^+\bar{\Lambda}_c^-$ was selected by reconstructing only a Λ_c^+ and an ISR photon $\gamma_{\rm ISR}$ to reserve as much as statistics. In this work, the Λ_c^+ baryon was reconstructed by combining the corresponding selected final states in the three Cabibbo-favored channels: $pK^-\pi^+$, pK_S^0 and $\Lambda\pi^+$, on which an exactly same mass window around Λ_c nominal mass was applied to reject the background events. In addition, to further suppress the combinatorial background, an anti-proton associating with $\bar{\Lambda}_c^-$ was required in each combination of $\gamma_{\rm ISR}\Lambda_c^+$. To select the signal events $e^+e^- \to \gamma_{\rm ISR}\Lambda_c^+\bar{\Lambda}_c^-$ exclusively, an asymmetric requirement window around the

nominal mass of Λ_c on the recoil mass against the combination $\gamma_{\rm ISR}\Lambda_c^+$ was imposed, which was defined as:

$$M_{\rm rec}(\gamma_{\rm ISR}\Lambda_c^+) = \sqrt{(\sqrt{s} - E_{\gamma_{\rm ISR}\Lambda_c^+})^2 - p^2_{\gamma_{\rm ISR}\Lambda_c^+}}, \quad (3)$$

where $E_{\gamma_{\rm ISR}\Lambda_c^+}$ and $p_{\gamma_{\rm ISR}\Lambda_c^+}$ are the total energy and momentum of the $\gamma_{\rm ISR}\Lambda_c^+$ combination, respectively. To measure the exclusive cross section of $e^+e^- \to \Lambda_c^+\bar{\Lambda}_c^-$ process, i.e., the $\Lambda_c^+\bar{\Lambda}_c^-$ invariant mass dependence of its production probability, the recoil mass spectrum against $\gamma_{\rm ISR}$, which was equivalent to $M(\Lambda_c^+\bar{\Lambda}_c^-)$, was extracted. In order to improve the resolution of $M(\Lambda_c^+\bar{\Lambda}_c^-)$ spectrum, the energy of ISR photon $\gamma_{\rm ISR}$ was corrected by constraining $M_{\rm rec}(\gamma_{\rm ISR}\Lambda_c^+)$ to the nominal mass of Λ_c.

Clear accumulation of events near the kinematic threshold in the $\Lambda_c^+\bar{\Lambda}_c^-$ invariant mass spectrum was observed by the authors, which was then fitted by a relativistic Breit–Wigner function. According to the fit result, the structure was parameterized with the mass $M = 4634^{+8}_{-7}(\text{stat})^{+5}_{-8}(\text{syst})$ MeV/c^2 and the total width $\Gamma_{\rm tot} = 92^{+40}_{-24}(\text{stat})^{+10}_{-21}(\text{syst})$ MeV. This resonance structure was found to be consistent within uncertainties with the previously observed 1^{--} charmonium-like state in the process $e^+e^- \to \pi\pi\psi(2S)$ [12]. The cross section line-shape of $e^+e^- \to \Lambda_c^+\bar{\Lambda}_c^-$ process was determined by correcting the background-subtracted $M(\Lambda_c^+\bar{\Lambda}_c^-)$ spectrum with the differential ISR luminosity and the detection efficiency function. As expected, the resonance structure led to a significant enhancement in the cross section near threshold. Due to the limited statistics, the polar angle distribution thereby the electromagnetic FFs of Λ_c^+ were not determined by the Belle collaboration.

3. The BESIII Measurement

Taking advantage of the large statistic energy scan data collected at c.m. energies $\sqrt{s} = 4574.5$, 4580.0, 4590.0 and 4599.5 MeV, the process $e^+e^- \to \Lambda_c^+\bar{\Lambda}_c^-$ is studied by BESIII both in the production cross section and electromagnetic form factor ratio [13], where the first energy is only 1.6 MeV above the kinematic threshold of $\Lambda_c^+\bar{\Lambda}_c^-$. Figure 2 illustrates a typical cascade process of the pair production and decay of Λ_c. To reserve as much as statistics, at each c.m. energy, a total of ten Cabibbo-favored hadronic decay modes as well as the ten corresponding charge-conjugate channels are independently used to singly reconstruct Λ_c^+ or $\bar{\Lambda}_c^-$. Each mode produces a cross-section result and the final cross section is obtained from a weighted average over the 20 individual measurements. The higher statistic data samples at the first and the last c.m. energies enable the study of the polar angle distribution of Λ_c in the c.m. system. The ratios between the electric and the magnetic FFs, i.e., $|G_E/G_M|$, are extracted for the first time.

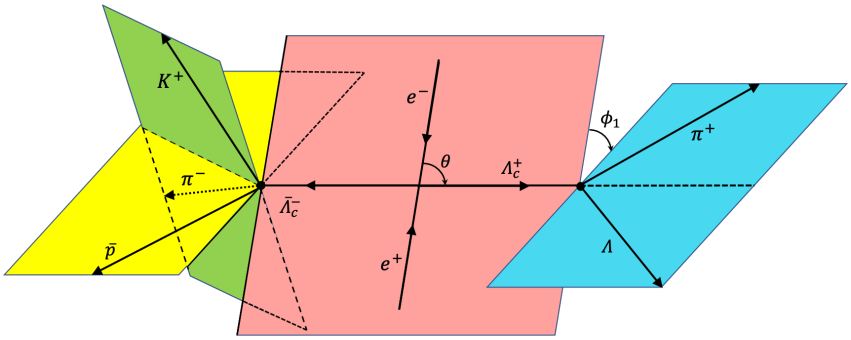

Figure 2. Pair production and decay of Λ_c in the annihilation of the electron–positron, where Λ_c^+ decays to the final state $\Lambda\pi^+$ while $\bar{\Lambda}_c^-$ to $\bar{p}K^+\pi^-$. The polar angle of outgoing Λ_c^+ is denoted by θ and the angle between the production and decay planes is illustrated by ϕ_1.

3.1. Cross Section Near Threshold

To extract the number of signal events in each Λ_c decay channel, the energy difference ΔE and the beam-constrained mass $M_{\rm BC}$, which reflect the energy and momentum conservation are utilized to identify the Λ_c signals. The energy difference is defined as $\Delta E \equiv E_{\Lambda_c} - E_{\rm beam}$, where E_{Λ_c} is the energy of the Λ_c candidate that is obtained by counting the energy of all the final state particles forming Λ_c and $E_{\rm beam}$ is the average energy of the two colliding beams. With each tagged mode, only the combination of Λ_c decay products with minimum $|\Delta E|$ is reserved. Since the involved c.m. energies are close to the kinematic threshold, no additional hadron is allowed to be produced associated with $\Lambda_c^+\bar{\Lambda}_c^-$ thereby ΔE peaks at zero. Events are further rejected if they are outside the dedicated ΔE requirement windows. The beam-constrained mass is defined as $M_{\rm BC} \equiv \sqrt{E^2_{\rm beam} - p^2_{\Lambda_c}}$, where p_{Λ_c} is the momentum of the Λ_c candidate. Similarly, there should be a peak around Λ_c^+ nominal mass in $M_{\rm BC}$ distribution. An un-binned maximum likelihood fit is performed on each $M_{\rm BC}$ distribution to determine the number of signal events with a specific decay pattern of Λ_c.

After correcting the number of signal events with the integrated luminosity of data sample, the vacuum polarization and ISR correction factors, the signal detection efficiency and the corresponding branching fractions [14], an individual measurement of the cross section of $e^+e^- \to \Lambda_c^+\bar{\Lambda}_c^-$ process is accomplished. The individual cross sections obtained at the same c.m. energy but in different decay channels are combined using the weighted average method described in Ref. [15], where the the averaging is performed over all 20 decay channels of the Λ_c^+ and $\bar{\Lambda}_c^-$ baryons. The total uncertainty of the average cross section is calculated after considering the correlations between any two individual cross sections. The average cross sections at the four c.m. energies are shown in Figure 3 together with the Belle data [11] for a comparison.

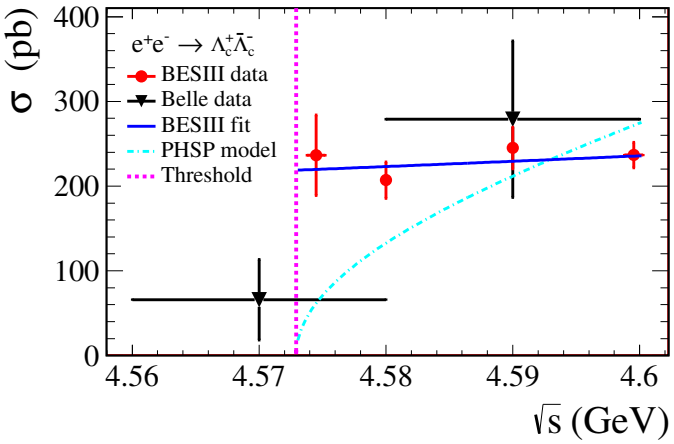

Figure 3. Cross section of $e^+e^- \to \Lambda_c^+\bar{\Lambda}_c^-$ measured by BESIII and Belle collaborations [13]. The blue solid curve is a phenomenological fit of the BESIII data while the dash-dot cyan curve denotes the prediction of the trivial phase space model, which is parameterized by Equation (2) but with the unity Coulomb factor and constant $|G_M|$.

3.2. Ratio of the Electric and Magnetic form Factors

Based on the relatively larger integrated luminosity at BESIII, the polar angle distributions of process $e^+e^- \to \Lambda_c^+\bar{\Lambda}_c^-$ in its c.m. frame are also studied at $\sqrt{s}$ = 4574.5 and 4599.5 MeV, respectively. The polar angle of Λ_c is defined as θ in Figure 2, and the polar angle distribution is actually the differential production cross section in terms of $\cos\theta$. To determine $\cos\theta$ dependence of signal yields, $\cos\theta$ of Λ_c are divided into ten equivalent bins considering the limited statistics. The $\cos\theta$ value of each $e^+e^- \to \Lambda_c^+\bar{\Lambda}_c^-$ event is calculated by $\cos\theta = p_{z,\Lambda_c^+}/p_{\Lambda_c^+}$, where p_{z,Λ_c^+} is the momentum along the beam direction of Λ_c^+. Similar with the case in cross-section measurement, the number of signal events in

each $\cos\theta_{\Lambda_c^+}$ bin is determined by fitting the corresponding $M_{\rm BC}$ distributions. For better statistics, the signal events in the same $\cos\theta_{\Lambda_c^+}$ bin but from different tagged decay modes are combined. After applying one-dimensional bin-by-bin efficiency corrections on these total yields, the authors have obtained the polar angle distributions at the two c.m. energies by tagging Λ_c^+. To further reduce the statistical uncertainty of the polar angle shape parameter, the same procedure is performed by tagging the $\bar{\Lambda}_c^-$ decays, and the combined polar angle distribution of $e^+e^- \to \Lambda_c^+\bar{\Lambda}_c^-$ process at each c.m. energy is obtained by combining the corresponding distributions of Λ_c^+ and $\bar{\Lambda}_c^-$ bin-by-bin. The probability function $\mathcal{P}(\theta) \propto (1 + \alpha_{\Lambda_c}\cos^2\theta)$ is used to fit the combined polar angle distribution, which is illustrated in Figure 4.

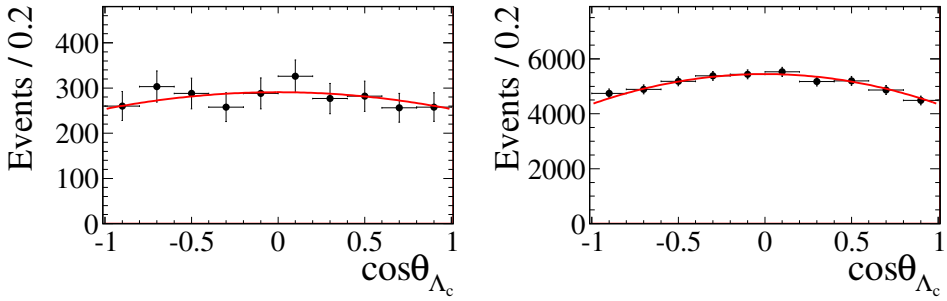

Figure 4. Polar angle distributions and results of the fit to data at $\sqrt{s}$ = 4574.5 MeV (**left**) and 4599.5 MeV (**right**), where the fit function $1 + \alpha_{\Lambda_c}\cos^2\theta$ is shown in red curves [13].

After determining the shape parameters α_{Λ_c}, the $|G_E/G_M|$ ratios is extracted using the equation

$$|G_E/G_M|^2(1-\beta^2) = (1-\alpha_{\Lambda_c})/(1+\alpha_{\Lambda_c}). \quad (4)$$

where β is the velocity of the out-going Λ_c^+ as defined in Equation (1). At BESIII, $|G_E/G_M|$ of Λ_c^+ are determined for the first time to be $1.14 \pm 0.14 \pm 0.07$ and $1.23 \pm 0.05 \pm 0.03$ at $\sqrt{s} = 4574.5$ and 4599.5 MeV, respectively. It is found that $|G_E/G_M|$ at the c.m. energy closest to the kinematic threshold is consistent with 1 within the uncertainty.

3.3. The Relative Phase between Electric and Magnetic Form Factors

If the electric and magnetic form factors of baryon in the time-like domain are different, they have a non-zero phase [4,16]. In the process $e^+e^- \to B\bar{B}$ where B is a baryon, the non-vanishing phase between G_E and G_M introduces polarization effects to the baryon B, even if initial state is unpolarized [16]. Different from the case for the nucleons, if the baryon B is a strange or charmed hyperon, the polarization of B is experimentally accessible due to the weak, parity violation decays of B [17].

Thanks to the recent completely developed helicity formalism of the weak two-body hadronic decay of hyperons produced by electron–positron annihilations [18], the BESIII collaboration has also studied the transverse polarization of Λ_c^+ in unpolarized electron–positron collisions for the first time [19]. In this measurement, a total of 567 pb^{-1} data samples collected at $\sqrt{s} = 4599.5$ MeV are analyzed. For better statistics, four two-body decay channels of Λ_c^+: pK_S^0, $\Lambda\pi^+$, $\Sigma^+\pi^0$ and $\Sigma^0\pi^+$ are used to probe the transverse polarization of Λ_c^+, which is defined as

$$P_T(\cos\theta) = \sqrt{1-\alpha_{\Lambda_c}^2}\cos\theta\sin\theta\sin\Delta\Phi, \quad (5)$$

where $\Delta\Phi$ is the relative phase between the electric and magnetic form factors of Λ_c^+, while θ and α_{Λ_c} are the polar angle and shape parameter of the polar angle distribution shared by the four decay channels, respectively. With a simultaneous un-binned maximum likelihood fit on the four data sets, the relative phase between G_E and G_M is extracted to be $\sin\Delta\Phi = -0.28 \pm 0.13 \pm 0.03$ with a statistical significance of 2.1 standard deviations.

4. Discussion and Conclusions

Based on the rigorously conducted measurement of the process $e^+e^- \to \Lambda_c^+\bar{\Lambda}_c^-$ by the Belle collaboration [11], theoretic interpretations of the pair production mechanism of Λ_c^+ is proposed and discussed [20–22]. Since a clear resonance structure, which is named as $X(4630)$ by the authors, is observed in the corresponding cross-section line-shape. The $X(4630)$ structure is consistent with the charmonium-like state $Y(4660)$, which is observed in the process $e^+e^- \to \pi^+\pi^-\psi(2S)$ [12]. With a combined fit of cross-section data in $\Lambda_c^+\bar{\Lambda}_c^-$ and $\pi^+\pi^-\psi(2S)$ process, it is concluded that these two structures originated from the same resonance, which is identified as a *Charmed Baryonium* [21]. According to its large baryon decay rate by comparing that to $\pi^+\pi^-\psi(2S)$, the authors believe that this state is an excellent candidate for a $[cq][\bar{c}\bar{q}]$ diquark–antidiquark bound state, which is connected by a string neutralizing their color. The decay of this state to $\Lambda_c^+\bar{\Lambda}_c^-$ is a result of the breaking of the string. The authors also exclude any baryon molecule interpretation due to the fact that this structure is sensibly higher than the baryon–antibaryon threshold. In Ref. [22], it is demonstrated that the enhancement in $e^+e^- \to \Lambda_c^+\bar{\Lambda}_c^-$ cross section measured by Belle could be consistent with the $\psi(2S)f_0(980)$ molecular picture of $Y(4660)$ taking into account the $\Lambda_c^+\bar{\Lambda}_c^-$ final state interaction.

To further study the connection between $X(4630)$ in final state $\Lambda_c^+\bar{\Lambda}_c^-$ and $Y(4660)$ in $\pi^+\pi^-\psi(2S)$, a more rigorous investigation of the $e^+e^- \to \Lambda_c^+\bar{\Lambda}_c^-$ process close to the threshold is performed in Ref. [23]. In this work, except the standing resonance $X(4630)$, a relevant final state interaction in the $\Lambda_c^+\bar{\Lambda}_c^-$ system was constructed based on the lines of chiral effective field theory up to next-to-leading order, in which the inherent parameters are determined by a fit to the Belle measured $e^+e^- \to \Lambda_c^+\bar{\Lambda}_c^-$ data. After taking the interplay between $X(4630)$ and the final state interaction in $\Lambda_c^+\bar{\Lambda}_c^-$ system into consideration, the authors have obtained the resonance parameters of $X(4630)$ with improved precision and conclusively confirmed the conjecture that the structures $X(4630)$ and $Y(4660)$ are the same state. However, exploratory fits with the same model can not reconcile the different trends for the c.m. energy dependence of the $e^+e^- \to \Lambda_c^+\bar{\Lambda}_c^-$ cross sections between Belle and BESIII. The authors state that the drastic impact on the resonance parameters of $X(4630)$ will be produced if the energy dependence trend of BESIII data persists for higher energies, as indicated by Figure 5.

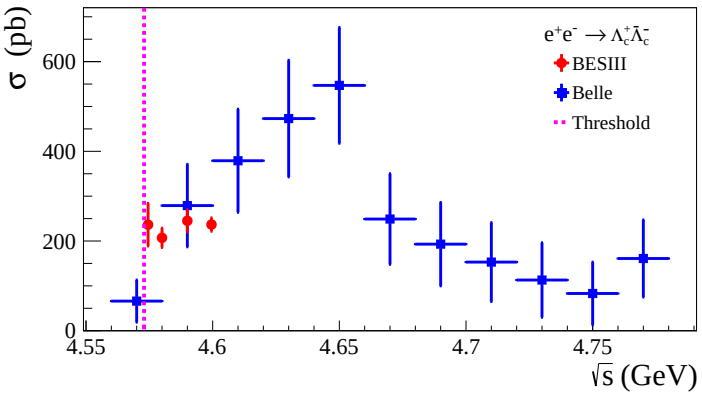

Figure 5. Different energy dependent trends of the resulting $e^+e^- \to \Lambda_c^+\bar{\Lambda}_c^-$ cross sections between BESIII and Belle.

After the BESIII collaboration provided the cross sections of $e^+e^- \to \Lambda_c^+\bar{\Lambda}_c^-$ process in the proximity of the threshold with unprecedented precision [13], theoretic models are proposed to incorporate the BESIII measurements with that of Belle [24–26].

In addition to the $X(4630)$ resonance structure, a virtual pole generated by $\Lambda_c^+\bar{\Lambda}_c^-$ attractive final state interaction is suggested by Ref. [24] to explain the enhanced cross section right above the $\Lambda_c^+\bar{\Lambda}_c^-$ threshold. This pole is regarded as a $\Lambda_c^+\bar{\Lambda}_c^-$ molecular virtual state and would become a bound state if $\Lambda_c^+\bar{\Lambda}_c^-$ contact coupling were larger. The good

fit quality to the data of this combined model suggests the existence of the virtual pole with statistical significance of 4.2 standard deviation. In addition, with the resonance structure $X(4630)$ described by the Breit–Wigner function, the continuum contribution, which is motivated by the cross section data of $e^+e^- \to p\bar{p}$ and $\Lambda\bar{\Lambda}$ processes, is introduced by Ref. [25] to fit the combined cross section data from BESIII and Belle. Again, good agreement between the model and cross-section data is achieved; however, the nature of the continuum part is not clearly understood.

The modified vector meson dominance (VMD) model is developed by Ref. [26] to parameterize the Dirac and Pauli form factors of Λ_c^+, in which the contributions from the intrinsic structure as well as the meson clouds parts are included. Since the charmed baryon Λ_c^+ is a isoscalar, the contributions from the isovector mesons are excluded when constructing the VMD model. The electromagnetic FFs of Λ_c^+ are obtained by the linear combination of the established Dirac and Pauli FFs, then the $e^+e^- \to \Lambda_c^+\bar{\Lambda}_c^-$ cross sections measured by the Belle and BESIII collaborations are simultaneously fitted with Equation (2). With the parameters determined by the fit, the authors predicted c.m. energy dependence of a variety of observables related with the electromagnetic FFs of Λ_c^+, including $|G_E/G_M|$, the relative phase between G_E and G_M and the polarization observables of Λ_c^+. Measurement of these observables can examine the validity of the modified VMD model.

5. Summary and Prospect

As a natural analogy to proton, Λ_c^+ is the lightest charged baryon that contains a charm quark. Experimental measurements of the production and decay properties of Λ_c^+ could definitely provide crucial information for the study of both strong and weak interactions; however, the current measurement of Belle suffers from relatively large uncertainty and that of BESIII is limited in a small c.m. energy region near threshold. Therefore, to further resolve the tension between the $e^+e^- \to \Lambda_c^+\bar{\Lambda}_c^-$ cross section line-shapes measured by Belle and BESIII, clarify the puzzle related with $X(4630)$ and $Y(4660)$ mesons and validate the scenarios describing the production mechanism and internal structure of charmed baryon Λ_c^+, precision measurements of the cross section as well as the polar angle distributions of process $e^+e^- \to \Lambda_c^+\bar{\Lambda}_c^-$ in higher energies at BESIII or other facilities such as Belle II are highly desired.

The Belle II collaboration will accumulate data corresponds to an integrated luminosity of 50 ab^{-1} in the following years [27], which will definitely help to re-examine the pair production of Λ_c^+ via the ISR technique. Currently, the BESIII detector has collected scan data at fourteen c.m. energies from 4.61 to 4.95 GeV with relatively large statistics [28]. Based on these data sets, it is possible that a high precision production cross-section line-shape will be produced. In addition, by analyzing the polar angle distribution and the helicity angles of the cascade decays of Λ_c^+, even the energy dependent ratio as well as relative phase angle between the electric and magnetic form factors of Λ_c^+ can be extracted at BESIII. Anyway, it is worth anticipating that more experimental information will be available in the near future to greatly improve the knowledge about the production mechanism of the charmed baryon Λ_c^+.

Author Contributions: Conceptualization, W.W., R.B.F. and G.H.; Formal analysis, W.W.; Funding acquisition, G.H.; Investigation, W.W.; Methodology, W.W.; Supervision, X.Z., R.B.F. and G.H.; Validation, X.Z.; Writing—original draft, W.W.; Writing—review & editing, W.W. and G.H. All authors have read and agreed to the published version of the manuscript.

Funding: This work is supported in part by National Key Research and Development Program of China under Contracts No. 2020YFA0406403; National Natural Science Foundation of China (NSFC) under Contract Nos. 12035013, 12061131003, 11335008; China Postdoctoral Science Foundation grant numbers 2019M662152, 2020T130636; Fundamental Research Funds for the Central Universities grant number WK2030000053.

Institutional Review Board Statement: Not applicable.

Informed Consent Statement: Not applicable.

Data Availability Statement: Not applicable.

Acknowledgments: Authors thank the guest editors: Monica Bertani, Simone Pacetti and Alessio Mangoni for their kind invitations and helps. Authors also thank Xiongfei Wang for his careful reading of this paper.

Conflicts of Interest: The authors declare no conflict of interest.

References

1. Punjabi, V.; Perdrisat, C.F.; Jones, M.K. The structure of the nucleon: Elastic electromagnetic form factors. *Eur. Phys. J. A* **2015**, *51*, 79. [CrossRef]
2. Huang, G.S.; Baldini Ferroli, R. Probing the internal structure of baryons. *Natl. Sci. Rev.* **2021**, nwab187. [CrossRef] [PubMed]
3. Cabibbo, N.; Gatto, R. Electron-Positron Colliding Beam Experiments. *Phys. Rev.* **1961**, *124*, 1577. [CrossRef]
4. Pacetti, S.; Baldini Ferroli, R.; Tomasi-Gustafsson, E. Proton electromagnetic form factors: Basic notions, present achievements and future perspectives. *Phys. Rep.* **2015**, *550–551*, 1–103. [CrossRef]
5. Sommerfeld, A. Über die Beugung und Bremsung der Elektronen. *Ann. Phys.* **1931**, *403*, 257. [CrossRef]
6. Brodsky, S.J.; Lebed, R.F. Production of the Smallest QED Atom: True Muonium ($\mu^+\mu^-$). *Phys. Rev. Lett.* **2009**, *102*, 213401. [CrossRef] [PubMed]
7. Sakharov, A.D. Interaction of the electron and the positron in pair production. *Sov. Phys. Usp.* **1991**, *34*, 375. [CrossRef]
8. Cazzoli, E.G.; Cnops, A.M.; Connolly, P.L.; Louttit, R.I.; Murtagh, M.J.; Palmer, R.B.; Samios, N.P.; Tso, T.T.; Williams, H.H. Evidence for $\Delta S = -\Delta Q$ Currents or Charmed-Baryon Production by Neutrinos. *Phys. Rev. Lett.* **1975**, *34*, 1125. [CrossRef]
9. Knapp, B.; Lee, W.; Smith, S.D.; Wijangco, A.; Knauer, J.; Yount, D.; Bronstein, J.; Coleman, R.; Gladding, G.; Goodman, M.; et al. Observation of a Narrow Antibaryon State at 2.26 GeV/c^2. *Phys. Rev. Lett.* **1976**, *37*, 882. [CrossRef]
10. Abrams, G.S.; Alam, M.S.; Blocker, C.A.; Boyarski, A.M.; Breidenbach, M.; Burke, D.L.; Carithers, W.C.; Chinowsky, W.; Coles, M.W.; Cooper, S.; et al. Observation of Charmed-Baryon Production in e^+e^- Annihilation. *Phys. Rev. Lett.* **1980**, *44*, 10. [CrossRef]
11. Pakhlova, G.; Adachi, I.; Aihara, H.; Arinstein, K.; Aulchenko, V.; Aushev, T.; Bakich, A.M.; Balagura, V.; Bedny, I.; Bhardwaj, V.; et al. (Belle Collaboration), Observation of a Near-Threshold Enhancement in the $e^+e^- \to \Lambda_c^+\bar{\Lambda}_c^-$ Cross Section Using Initial-State Radiation. *Phys. Rev. Lett.* **2008**, *101*, 172001. [CrossRef]
12. Wang, X.L.; Yuan, C.Z.; Shen, C.P.; Wang, P.; Adachi, I.; Aihara, H.; Arinstein,K.; Aushev,T.; Barberio, E.; Bedny, I.; et al. (Belle Collaboration), Observation of Two Resonant Structures in $e^+e^- \to \pi^+\pi^-\psi(2S)$ via Initial-State Radiation at Belle. *Phys. Rev. Lett.* **2007**, *99*, 142002. [CrossRef]
13. Ablikim, M.; Achasov, M.N.; Ahmed, S.; Albrecht, M.; Alekseev, M.; Amoroso, A.; An, F.F.; An, Q.; Bai, J.Z.; Bai, Y.; et al. (BESIII Collaboration), Precision Measurement of the $e^+e^- \to \Lambda_c^+\bar{\Lambda}_c^-$ Cross Section Near Threshold. *Phys. Rev. Lett.* **2018**, *120*, 132001. [CrossRef] [PubMed]
14. Ablikim, M.; Achasov, M.N.; Ai, X.C.; Albayrak, O.; Albrecht, M.; Ambrose, D.J.; Amoroso, A.; An, F.F.; An, Q.; Bai, J.Z.; et al. (BESIII Collaboration), Measurements of Absolute Hadronic Branching Fractions of the Λ_c^+ Baryon. *Phys. Rev. Lett.* **2016**, *116*, 052001. [CrossRef] [PubMed]
15. Schmelling, M. Averaging correlated data. *Phys. Scr.* **1995**, *51*, 676. [CrossRef]
16. Dubnickova, A.Z.; Dubnicka, S.; Rekalo, M.P. Investigation of the baryon electromagnetic structure by polarization effects in $e^+e^- \to B\bar{B}$ processes. *Nuovo Cimento A* **1996**, *109*, 241. [CrossRef]
17. Ablikim, M.; Achasov, M.N.; Adlarson, P.; Ahmed, S.; Albrecht, M.; Alekseev, M.; Amoroso, A.; An, F.F.; An, Q.; Bai, Y.; et al. (BESIII Collaboration), Complete Measurements of the Λ Electromagnetic Form Factors. *Phys. Rev. Lett.* **2019**, *123*, 122003. [CrossRef] [PubMed]
18. Perotti, E.; Fäldt, G.; Kupsc, A.; Leupold, S.; Song, J.J. Polarization observables in e^+e^- annihilation to a baryon-antibaryon pair. *Phys. Rev. D* **2019**, *99*, 056008. [CrossRef]
19. Ablikim, M.; Achasov, M.N.; Adlarson, P.; Ahmed, S.; Albrecht, M.; Alekseev, M.; Amoroso, A.; An, F.F.; An, Q.; Bai, Y.; et al. (BESIII Collaboration), Measurements of weak decay symmetries of $\Lambda_c^+ \to pK_S^0$, $\Lambda\pi^+$, $\Sigma^+\pi^0$ and $\Sigma^0\pi^+$. *Phys. Rev. D* **2019**, *100*, 072004. [CrossRef]
20. Bugg, D.V. An alternative fit to Belle mass spectra for $D\bar{D}$, $D^*\bar{D}^*$ and $\Lambda_c\bar{\Lambda}_c$. *J. Phys. G: Nucl. Part. Phys.* **2009**, *36*, 075002. [CrossRef]
21. Cotugno, G.; Faccini, R.; Polosa, A.D.; Sabelli, C. Charmed Baryonium. *Phys. Rev. Lett.* **2010**, *104*, 132005. [CrossRef]
22. Guo, F.K.; Haidenbauer, J.; Hanhart, C.; Meißner, U.G. Reconciling the $X4630$ with the $Y(4660)$. *Phys. Rev. D* **2010**, *82*, 094008. [CrossRef]
23. Dai, L.Y.; Haidenbauer, J.; Meißner, U.G. Re-examining the $X4630$ resonance in the reaction $e^+e^- \to \Lambda_c^+\bar{\Lambda}_c^-$. *Phys. Rev. D* **2017**, *96*,116001. [CrossRef]
24. Cao, Q.F.; Qi, H.R.; Wang, Y.F.; Zheng, H.Q. Discussion on the line-shape of the $X(4660)$ resonance. *Phys. Rev. D* **2019**, *100*, 054040. [CrossRef]
25. Xie, Y.; Liu, Z.Q. Exploring the $e^+e^- \to \Lambda_c^+\bar{\Lambda}_c^-$ cross Sections. *arXiv* **2020**. Available online: https://arxiv.org/pdf/2001.09620.pdf (accessed on 13 December 2021).

26. Wan, J.Y.; Yang, Y.L.; Lu, Z. The Electromagnetic Form Factors of Λ_c Hyperon in the Vector Meson Dominance Model. *arXiv* **2019**. Available online: https://arxiv.org/pdf/2102.03092.pdf (accessed on 13 December 2021).
27. Kou, E.; Urquijo, P.; Altmannshofer, W.; Beaujean, F.; Bell, G.; Beneke, M.; Bigi, I.I.; Bishara, F.; Blanke, M.; Bobeth, C.; et al. The Belle II Physics Book. *Prog. Theor. Exp. Phys.* **2019**, *123C01*. [CrossRef]
28. Ablikim, M.; Achasov, M.N.; Adlarson, P.; Ahmed, S.; Albrecht, M.; Alekseev, M.; Amoroso, A.; An F.F.; An Q.; Bai, Y.; et al. (BESIII Collaboration), Future Physics Programme of BESIII. *Chin. Phys. C* **2020**, *44*, 040001. [CrossRef]